Author Manuscript

Author Manuscript

Author Manuscript

Author Manuscript

HHS Public Access

Author manuscript

Mod Pathol. Author manuscript; available in PMC 2020 September 11.

Published in final edited form as:

Mod Pathol. 2018 August ; 31(8): 1246–1256. doi:10.1038/s41379-018-0045-3.

Array-based DNA-methylation profiling in sarcomas with small blue round cell histology provides valuable diagnostic information

Christian Koelsche[1,2,3], **Wolfgang Hartmann**[4], **Daniel Schrimpf**[1,2,3], **Damian Stichel**[1,3], **Susanne Jabar**[5,6,7], **Andreas Ranft**[5,6,7], **David E. Reuss**[1,2,3], **Felix Sahm**[1,2,3], **David T.W. Jones**[3,8,9], **Melanie Bewerunge-Hudler**[3,10], **Marcel Trautmann**[4], **Thomas Klingebiel**[11], **Christian Vokuhl**[12], **Manfred Gessler**[13,14], **Eva Wardelmann**[4], **Iver Petersen**[15], **Daniel Baumhoer**[16], **Uta Flucke**[17], **Cristina Antonescu**[18], **Manel Esteller**[19,20,21], **Stefan Fröhling**[3,22,23], **Marcel Kool**[3,8,9], **Stefan M. Pfister**[3,8,9], **Gunhild Mechtersheimer**[24], **Uta Dirksen**[5,6,7,*], **Andreas von Deimling**[1,2,3,*]

[1.]Clinical Cooperation Unit Neuropathology, German Cancer Research Center (DKFZ), Heidelberg, Germany [2.]Department of Neuropathology, Institute of Pathology, Heidelberg University Hospital, Heidelberg, Germany [3.]German Cancer Consortium (DKTK), Core Center Heidelberg, Germany [4.]Gerhard Domagk Institute of Pathology, Muenster University Hospital, Muenster, Germany [5.]Pediatrics III Pediatric Hematology, Oncology, Immunology, Cardiology, Pulmonology, West German Cancer Centre, University Hospital Essen, Essen, Germany [6.]German Cancer Consortium (DKTK), Center Essen, Germany [7.]Sarcoma Center, International Ewing Sarcoma Study Group, West German Cancer Center, University Duisburg-Essen, Essen, Germany [8.]Center for Individualized Pediatric Oncology (ZIPO) and Brain Tumors, Heidelberg, Germany [9.]Division of Pediatric Neurooncology, German Cancer Consortium (DKTK), German Cancer Research Center (DKFZ), Heidelberg, Germany [10.]Genomics and Proteomics Core Facility, German Cancer Research Center (DKFZ), Heidelberg, Germany [11.]Department of Pediatric Hematology and Oncology, University Children's Hospital, Frankfurt/Main, Germany [12.]Department of Pediatric Pathology, University Hospital of Schleswig-Holstein, Kiel, Germany [13.]Theodor-Boveri-Institute/Biocenter, Developmental Biochemistry, Wuerzburg University, Wuerzburg, Germany [14.]Comprehensive Cancer Center Mainfranken, Wuerzburg University, Wuerzburg, Germany [15.]Institute of Pathology, SRH Poliklinik Gera GmbH, Gera, Germany [16.]Bone Tumour Reference Centre, Institute of Pathology, Basel University Hospital, Basel, Switzerland [17.]Department of Pathology, Radboud University Medical Center, Nijmegen, The

Corresponding Author: Prof. Dr. med. Andreas von Deimling, University Hospital Heidelberg, Department of Neuropathology, Im Neuenheimer Feld 224, 69120 Heidelberg, Germany, Fon: +49 (0)6221 56 4650, Fax: +49 (0)6221 56 4566, andreas.vondeimling@med.uni-heidelberg.de ; Prof. Dr. med Uta Dirksen, University Hospital Essen, Pediatrics III, Hematology/Oncology, Sarcoma Centre, International Ewing Sarcoma Study Group, West German Cancer Centre, Hufelandstr. 55, 45147 Essen, Germany, Fon: +49 (0)201 723 3784, Fax: +49 (0)201 723 5386, uta.dirksen@uk-essen.de.

*equal contribution

Financial disclosure
Nothing to declare.

Competing interests
Nothing to declare.

Supplementary information is available at *Modern Pathology*'s website

Author Manuscript Author Manuscript Author Manuscript Author Manuscript

Netherlands [18]Department of Pathology, Memorial Sloan Kettering Cancer Center, New York, United States of America [19]Cancer Epigenetics and Biology Program (PEBC), Bellvitge Biomedical Research Institute (IDIBELL), Barcelona, Catalonia, Spain [20]Department of Physiological Sciences II, School of Medicine, University of Barcelona, Barcelona, Catalonia, Spain [21]Institucio Catalana de Recerca i Estudis Avançats (ICREA), Barcelona, Catalonia, Spain [22]Department of Translational Oncology, National Center for Tumor Diseases (NCT) Heidelberg and German Cancer Research Center (DKFZ), Heidelberg, Germany [23]Section for Personalized Oncology, Heidelberg University Hospital, Heidelberg, Germany [24]Department of General Pathology, Institute of Pathology, Heidelberg University Hospital, Heidelberg, Germany

Abstract

Undifferentiated solid tumors with small blue round cell histology and expression of CD99 mostly resemble Ewing sarcoma, however, also may include other tumors such as mesenchymal chondrosarcoma, synovial sarcoma or small cell osteosarcoma. Definitive classification usually requires detection of entity-specific mutations. While this approach identifies the majority of Ewing sarcomas, a subset of lesions remains unclassified and, therefore, has been termed “Ewing-like sarcomas” or small blue round cell tumors not otherwise specified. We developed an approach for further characterization of small blue round cell tumors not otherwise specified using an array-based DNA-methylation profiling approach. Data were analyzed by unsupervised clustering and t-distributed stochastic neighbor embedding analysis and compared with a reference methylation data set of 460 well-characterized prototypical sarcomas encompassing 18 subtypes. Verification was performed by additional FISH-analyses, RNA-sequencing from formalin-fixed paraffin-embedded material or immunohistochemical marker analyses. In a cohort of more than 1,000 tumors assumed to represent Ewing sarcomas, 30 failed to exhibit the typical EWS translocation. These tumors were subjected to methylation profiling and could be assigned to Ewing sarcoma in 14 (47%), to small blue round cell tumors with *CIC* alteration in 6 (20%), to small blue round cell tumors with *BCOR* alteration in 4 (13%), to synovial sarcoma and to malignant rhabdoid tumor in 2 cases each. One single case each was allotted to mesenchymal chondrosarcoma and adamantinoma. 12/14 tumors classified as Ewing sarcoma could be verified by demonstrating either a canonical EWS translocation evading initial testing, by identifying rare breakpoints or fusion partners. The methylation based assignment of the remaining small blue round cell tumors not otherwise specified also could be verified by entity-specific molecular alterations in 13/16 cases. In conclusion, array-based DNA-methylation analysis of undifferentiated tumors with small blue round cell histology is a powerful tool for precisely classifying this diagnostically challenging tumor group.

Keywords

Ewing-like; EWING; small blue round cell tumors; CIC; BCOR; EPIC; methylation

Author Manuscript Author Manuscript Author Manuscript Author Manuscript

Introduction

Ewing sarcoma is a highly malignant tumor that accounts for approximately 8 % of all bone tumors. Although Ewing sarcoma is a rare disease, it represents the second most common malignant bone tumor in children and adolescents with a peak incidence in the second decade of life (1). Ewing sarcoma is a prototypical example for an undifferentiated sarcoma with small blue round cell phenotype, which, however, is shared with several other sarcoma entities. Unfortunately, expression of CD99, typical for Ewing sarcoma, is also encountered in several morphological mimics. Therefore, it is not sufficient diagnosing Ewing sarcomas based on histologic criteria and immunohistochemical marker expression alone (2).

A breakthrough in the diagnostics of Ewing sarcoma was the discovery of two highly specific translocations, which both result in a gene fusion between a member of the *TET*- and *ETS*- gene families. The two most common translocations in Ewing sarcoma either lead to a chimeric gene fusion between *EWSR1-FLI1* or *EWSR1-ERG* seen in approximately 85-90 % and 5-10 % of all cases, respectively (3, 4). Gene fusions with other *TET* and *ETS* family members and rearrangements of *EWSR1* with non-*ETS* family genes have also been described. However, such fusions are exceptionally rare occurring in less than 1 % of Ewing sarcomas (5, 6).

Molecular analysis of Ewing sarcomas and mimics sharing histological and clinical features by extended FISH analysis and next generation sequencing has separated Ewing sarcomas with canonical translocations from so-called “Ewing-like” sarcomas. Subgroups of “Ewing-like” sarcomas carry a *CIC-DUX4* or a *BCOR-CCNB3* gene fusion or other specific molecular alterations (7-10). However, frequently “Ewing-like” sarcomas remain molecularly undefined due to the rarity and/or diversity of the discriminating molecular features and the lack of established routine techniques to detect them. These tumors usually are placed with a basket category termed small blue round cell tumors not otherwise specified (11).

The methylation status of gene promoters is a strong indicator of the differentiation status along cell lineages (12, 13). Interestingly, this approach has also been shown very useful in distinguishing the tumor cell origin in a lineage dependent manner (14). Moreover, this approach allows molecular classification within seemingly morphological homogenous entities (15-23). The considerable stability of epigenetic signatures during tumor disease has been demonstrated for many tumors (18, 24, 25). Thus, determination of DNA-methylation signatures may also be useful for addressing “Ewing-like” sarcomas or small blue round cell tumors not otherwise specified.

In the present study we aimed at characterization of 30 sarcomas believed to represent Ewing sarcomas but not exhibiting the canonical EWS translocations at initial testing by reference pathology.

Author Manuscript Author Manuscript Author Manuscript Author Manuscript

Material and Methods

Sample selection

The 30 samples, all from different patients, were identified from a series of more than 1,000 patients referenced in the cooperative *Ewing's* sarcoma study (CESS) centre in Germany (26-28). Clinical characteristics are given in Supplementary Table S1. The CESS reference pathology in Muenster tested these samples negative for a translocation between *EWSR1* with either *FLI1* or *ERG* by applying RT-PCR that covered the most common fusion breakpoints. The diagnostic repertoire has been expanded to *EWSR1*- and *FUS*-break-apart FISH since 2014. The reference set for building a framework of methylation groups comprised a total of 460 prototypical sarcoma cases from primary manifestations and metastases encompassing classic adamantinoma of the tibia with prominent epithelial component (n = 6), alveolar soft part sarcoma (n = 22), mesenchymal chondrosarcoma (n = 9), clear cell sarcoma of the kidney (n = 12), conventional osteosarcoma (n = 82), dermatofibrosarcoma protuberans (n = 39), desmoplastic small round cell tumor (n = 28), epithelioid sarcoma (n = 17), Ewing sarcoma carrying a gene fusion either between *EWSR1-FLI1* (n = 41), *EWSR1-ERG* (n = 3) or *FUS-ERG* (n = 1), or showing an *EWSR1* break-apart signal in the FISH test (n = 12), infantile fibrosarcoma (n = 13), malignant peripheral nerve sheath tumor (n = 22), malignant rhabdoid tumor (n = 18), embryonal rhabdomyosarcoma (n = 31), alveolar rhabdomyosarcoma (n = 33), small blue round cell tumor with *BCOR-CCNB3* fusion (n = 8), small blue round cell tumor with an rearrangement of *CIC* (n = 10), solitary fibrous tumor (n = 22) and synovial sarcoma (n = 31). Reference cases of genetically defined sarcoma subtypes were molecularly confirmed. The reference set also includes a control group composed of non-neoplastic reactive soft tissue (n = 10). The study was done in concordance with the guidelines set forth by the local ethics committee of the University of Heidelberg and Muenster.

Genomic DNA and total RNA extraction

Representative formalin-fixed paraffin-embedded tumor tissue with highest available tumor content was chosen for extraction of RNA and DNA. Total cellular RNA was obtained using the Maxwell® 16FFPE Plus LEV RNA Kit and genomic DNA using the Maxwell® 16FFPE Plus LEV DNA Kit employing the automated Maxwell device (Promega, Madison, WI, USA) according to the manufacturer's instructions. The quality and concentration of RNA was determined on an Agilent 2100 Bioanalyzer® (Agilent Technologies, Santa Clara, CA, USA). DNA was quantified using the QuantiFast SYBR Green PCR Kit (Qiagen, Duesseldorf, NW, Germany).

Methylation Array data generation and pre-procession

The DNA-methylation status was obtained using the Illumina Infinium HumanMethylation450 (450k) array or the EPIC array (Illumina, San Diego, CA, USA), according to the manufacturer's instructions at the Genomics and Proteomics Core Facility of the DKFZ. DNA input quantity from formalin-fixed paraffin-embedded tumor material was 250ng (recommended by manufacturer). Equal data quality was obtained for DNA input down to 100ng (24). The turnaround time for the entire workflow starting with sample preparation, array processing, scanning and data analysis was approximately five working

Author Manuscript Author Manuscript Author Manuscript Author Manuscript

days. DNA-methylation data were normalized by performing background correction and dye bias correction shifting of negative control probe mean intensity to zero and scaling of normalization control probe mean intensity to 10,000, respectively. Probes targeting sex chromosomes and probes containing single nucleotide polymorphism that not uniquely matched were removed. In total, 438,370 probes contained on both, the 450k array and the EPIC array, were used for analysis.

Unsupervised clustering, copy number profiling and identification of differentially methylated regions

For unsupervised hierarchical clustering, we selected 10,000 probes that showed the highest standard deviation across the beta values. Samples were hierarchically clustered using the Pearson correlation coefficient as distance measure and average linkage. The CpGs were reordered using the Euclidian distance and complete linkage. For unsupervised 2D representation of pairwise sample correlations dimensionality reduction by t-distributed stochastic neighbor embedding was performed using the 20,000 most variable probes, a perplexity of 15 and 3,000 iterations. Copy number profiles were generated using the 'conumee' R package (http://www.bioconductor.org) and assessed manually.

Targeted RT-RNA and total RNA sequencing

The TruSeq RNA Access Library Prep Kit for formalin-fixed paraffin-embedded material (Illumina) was applied for total RNA sequencing according to the manufacturer's instructions. RNA libraries were sequenced on a NextSeq sequencer system (Illumina). Gene fusion transcripts were called from the RNA sequencing data using both deFuse and TopHat-Fusion algorithms (29, 30). If automated detection of gene fusions was negative, reads of candidate genes and their 3′ and 5′ intergenic neighborhood were manually investigated using the Integrative Genomics Viewer (IGV) (31). For targeted RNA sequencing the RNA was reverse transcribed and then subjected to PCR amplification using primer pairs covering the breakpoints of the common gene fusions of Ewing sarcoma (*EWSR1-FLI1*, *EWSR1-ERG*). *BCOR-CCNB3* rearrangements were detected by RT-PCR as well. Primer sequences are listed in Supplementary Table S2.

Fluorescent in Situ Hybridisation (FISH)

For interphase FISH, the slides were subjected to hybridization with the ZytoLight ® SPEC *EWSR1* dual color break apart probe, the ZytoLight ® SPEC *FUS* dual color break apart probe or the ZytoLight ® SPEC *SS18* dual color break apart probe (all ZytoVision, Bremerhafen, HB, Germany) according to the manufacturer's instructions. A *CIC* break apart assay was designed and performed using BAC clones RP11-374A11 and RP11-979P13 (Life Technologies, Carlsbad, CA, USA) essentially following protocols as described before (32). Hybridization signals were visualized with a DM5500 fluorescence microscope (Leica, Wetzlar, HE, Germany), and images were captured on a CCD camera.

Gene panel next generation sequencing

A customized SureSelect XT technology (Agilent) panel covering the coding regions of 130 genes, including *BCOR* and *CIC*, was applied to fusion negative cases where DNA-

Author Manuscript Author Manuscript Author Manuscript Author Manuscript

methylation profiling indicated a *BCOR or CIC* alteration. Library preparation, quality control, sequencing on a NextSeq sequencer (Illumina) and data processing were exactly performed as previously described (33). Reads were aligned against the reference genome hg19. Reads covering the *BCOR* locus (NM_001123383) were visualized in IGV and assessed manually for alterations.

Immunohistochemistry

A representative block was chosen for immunohistochemistry. 4-micron paraffin sections were dried at 80 °C for 15min and stained on a Ventana BenchMark XT immunostainer (Ventana Medical Systems, Tucson, AZ, USA) using standard techniques (Supplementary Table S3).

Results

Clinical features of the study cohort

30 CESS trial patients with the diagnosis of small blue round cell tumor not otherwise specified after histological and molecular evaluation by an expert panel of pathologists were subjected to DNA-methylation profiling. 26 cases were from the primary tumor, three from a metastatic tumor manifestation and one case from a recurrence. 18 patients were male, 12 were female. The median age at diagnosis was 17 (range 0 - 55) years. The primary manifestation site was skeletal in all but two cases. The majority of cases originated at the lower extremity (12/30), thoracic wall (6/30), pelvis (6/30), the upper extremity (4/30) and head and neck (2/30). Clinical data are compiled in Supplementary Table 1.

Epigenetic profiling assigned small blue round cell tumors not otherwise specified to distinct sarcoma subtypes

Genome-wide DNA-methylation profiles were generated of these 30 small blue round cell tumors not otherwise specified. Unsupervised clustering and t-distributed stochastic neighbor embedding analysis (Figure 1) together with 460 sarcomas from the reference series allotted the 30 small blue round cell tumors not otherwise specified to different methylation classes corresponding to sarcomas with a defined histology and characteristic molecular hallmarks: 14 (47 %) assigned to Ewing sarcoma, six (20 %) to small blue round cell tumors with *CIC* alteration, four (13 %) to small blue round cell tumors with *BCOR* alteration, which is a methylation group composed of small blue round cell tumors with *BCOR-CCNB3* fusion and clear cell sarcoma of the kidney with *BCOR* internal tandem duplication, two (7 %) to synovial sarcomas, two (7 %) to malignant rhabdoid tumors and one (3 %) to mesenchymal chondrosarcomas. Interestingly, one small blue round cell tumor not otherwise specified (3 %) clustered together with classic adamantinomas. Similar results were obtained when varying the number of CpGs used for the analysis (data not shown).

Genetic analyses validate the predicted sarcoma subtypes in most cases

To further validate the 30 small blue round cell tumors not otherwise specified, which by the DNA-methylation profiles were assigned to defined sarcoma subtypes, we analyzed these samples for molecular hallmark alterations. The results are compiled in Table 1. Cases falling into the Ewing sarcoma methylation class were tested by FISH, RT-PCR and total

Author Manuscript Author Manuscript Author Manuscript Author Manuscript

RNA sequencing. By applying this procedure, six of 14 tumors harbored a gene fusion between *EWSR1* and *FLI1*. The *EWSR1-FEV* fusion was detected once and so was the *EWSR1-ETV1* fusion. Four cases presented with a break-apart signal in the FISH analysis, three cases in *EWSR1* and one case in *FUS*. The gene fusion partner could not be further determined due to lack of sufficient tissue. In two cases, where material was only sufficient for FISH analysis, one case was negative for a break-apart signal in *EWSR1* or *FUS* and the other case was non-determinable.

Cases falling into the small blue round cell tumors with *CIC* alteration methylation class were tested by FISH and total RNA sequencing. Four of six tumors showed a *CIC* break-apart signal in the FISH analysis, indicating a rearrangement of the *CIC* locus. A *CIC-DUX4* fusion was revealed by RNA sequencing in two of them. Furthermore, RNA sequencing indicated a *CIC-DUX4* fusion in one of the two cases without a *CIC* break-apart signal.

Cases assigning to the methylation class small blue round cell tumors with *BCOR* alteration were tested by RT-PCR, total RNA sequencing and panel sequencing of the entire coding region if RNA-based methods were negative. Three of four tumors carried the *BCOR-CCNB3* fusion. In the fusion-negative case, a *BCOR* internal tandem duplication spanning 66 bases in exon 15 was detected (Figure 2).

Two tumors clustered with the methylation class for synovial sarcomas and were rearranged in the *SS18* locus. Histological re-evaluation lead to classification as poorly differentiated synovial sarcoma (Figure 3 A, B).

Two tumors clustered with the methylation class for malignant rhabdoid tumor and could be demonstrated to be *SMARCB1* deficient by copy number analysis and by INI-1 immunohistochemistry (Figure 3 C, D).

One tumor clustered with mesenchymal chondrosarcomas. Molecular testing by RNA sequencing did not reveal the *HEY1-NCOA2* fusion being expected in these malignancies. Cartilaginous areas or staghorn-shaped blood vessels, both frequent findings in mesenchymal chondrosarcomas, were absent in this case. Furthermore, the tumor was almost negative for S100 and CD99 expression (Figure 4).

One round cell tumor, which clustered together with adamantinomas, carried an *EWSR1-NFATC2* gene fusion. CD99 expression was faint, but yet recognizable positive. The copy number profile, which was calculated from the methylation array data, indicated a complex alteration on chromosome 22q (Figure 5). A very similar chromosome 22q alteration was found in one of the six classic adamantinomas. The histology of this particular case was unique compared with the other adamantinomas (Supplementary Figure S1). Unfortunately, the *EWSR1* break-apart FISH analysis failed in this case.

Discussion

The designations “Ewing-like” sarcoma or small blue round cell tumor not otherwise specified are highly unsatisfactory because they are employed in diagnostic settings having

Author Manuscript Author Manuscript Author Manuscript Author Manuscript

failed to produce unequivocal evidence for genetically defined sarcoma entities. Here, we demonstrated that methylation analysis is a powerful method, which assigns tumors currently named “Ewing-like” sarcoma and small blue round cell tumor not otherwise specified to well-defined diagnostic categories.

Validation analysis clearly supported the methylation based diagnostic assignment in 25 of 30 cases. In these, the detection of characteristic alterations was supportive for the prediction of the DNA-methylation-based analysis. It is noteworthy that methylation based assignment also correctly recognized sarcoma subtypes carrying exceedingly rare mutations, e.g. in Ewing sarcomas.

In only four cases, no characteristic alteration could be detected, probably due to the limitations of the applied methods. These four cases allotted to the methylation class Ewing sarcoma (n = 2), to small blue round cell tumors with *CIC* alteration (n = 1) and to mesenchymal chondrosarcoma (n = 1). In the latter case, the diagnosis could not be molecularly validated since it lacked the typical *HEY1-NCOA2* fusion described as a recurrent event in most, albeit not in all mesenchymal chondrosarcomas (34). Given the distinctive DNA-methylation signature in mesenchymal chondrosarcoma, we re-classified this case as mesenchymal chondrosarcoma with predominant small round cell component. In the two cases that assigned to the methylation class Ewing sarcoma, molecular validation was restricted to FISH analysis. The case matching with the methylation class small blue round cell tumors with *CIC* alteration had segmental copy number gains on chromosome arm 19q involving the *CIC* locus, which may have had an adverse effect on the FISH analysis (data not shown). Therefore, we consider it likely that DNA-methylation based prediction is also correct for those cases lacking the expected molecular alterations.

However, one outlier, which clustered in close proximity with classic adamantinomas of the tibia, surprisingly contained an *EWSR1-NFATC2* gene fusion. This uncommon fusion, first described in 2009, has yet been detected only in single bone tumors presenting with a phenotype similar to Ewing sarcoma (5, 11). Interestingly, the *EWSR1-NFATC2* gene fusion has also been described in one case with a hemangioma of the bone, although the breakpoint in *EWSR1* was more distal compared to the Ewing sarcoma-like cases (35). In the present case, the *EWSR1-NFATC2* breakpoint was matching with the one observed in Ewing sarcoma-like cases. The copy number profile of this tumor showed an unusual copy number alteration on chromosome 22q, which was also detected in one reference case classified as classic adamantinoma of the tibia. The histologic pattern of this reference case was well compatible with the histological features described in small blue round cell tumors carrying the *EWSR1-NFATC2* fusion (5, 11, 36). All of this makes not only the initial diagnosis of this particular reference case questionable, but also raise the question of the close epigenetic relation between *EWSR1-NFATC2* fused small blue round cell tumors and classic adamantinomas. The unusual “dot-like” cytokeratin expression pattern in *EWSR1-NFATC2* fused small blue round cell tumors might at least be suggestive of an epithelial differentiation similar to classic adamantinoma, which is characterized by a prominent epithelial cell component (36). However, we also cannot exclude a clustering artifact with absolute certainty. Thus, this case remained unsolved.

Author Manuscript Author Manuscript Author Manuscript Author Manuscript

Methylation based diagnostic assignment predicted four small blue round cell tumors with *BCOR* alteration. This methylation class is composed of different tumor subtypes sharing the molecular background of *BCOR* alteration either by rearrangement, internal tandem duplication or mutation. Small blue round cell tumors with *BCOR-CCNB3*, a sarcoma subtype probably being independent from the group of Ewing sarcoma, belongs to this methylation class (37). Accordingly, the *BCOR-CCNB3* fusion was detected in three cases (8, 10). The fourth case, an infant patient with a small blue round cell tumor in the skull, carried a *BCOR* internal tandem duplication. This case was re-classified as undifferentiated round cell sarcoma of infancy, in which the *BCOR* internal tandem duplication has been described as a highly recurrent event (38).

BCOR alterations have been recognized in a growing number of tumor subtypes affecting the soft tissue, the kidney or the central nervous system (22, 38, 39). Recent studies comparing the molecular and histologic phenotype in these *BCOR* altered tumors found overlapping features, especially between soft tissue and kidney tumors (38, 40, 41). At the level of DNA-methylation, we observed a great overlap in tumors from soft tissue and the kidney carrying *BCOR* alteration. Furthermore, using an extended set of tumor subtypes for DNA-methylation profiling (data not shown), also central nervous system high-grade neuroepithelial tumors with BCOR alteration fall into this methylation class (22). This is in line with the previously suggested concept that these tumors might constitute a family of tumors sharing *BCOR* alterations.

Overall, DNA-methylation profiling might potentially have clinical implications in the molecular diagnostics of small blue round cell tumors, as already seen in central nervous system tumors (22, 25). Four recently published studies observed misleading results of molecular tests widely used in the diagnostics of small blue round cell tumors. A deletion of the *SMARCB1* locus on chromosome arm 22q, which located juxtaposed to the *EWSR1* locus, can result in a false-positive *EWSR1* break-apart FISH signal, although the gene integrity is retained (42). Decision-making might further be impeded by false negative results in the molecular testing of small blue round cell tumors with *CIC* alteration (9, 43-45). Two recent articles focused on the performance of molecular tests in small blue round cell tumors with *CIC* rearrangement observed an overall low performance of break-apart FISH and total RNA sequencing in these tumors (46, 47). Their results reflect our experience with molecular testing in small blue round cell tumors with *CIC* alteration. We could demonstrate a *CIC* rearrangement in four of six cases by break-apart FISH analysis. Copy number profiling of the two break-apart negative cases revealed complex alterations involving the *CIC* locus on chromosome 19q, which may have had an adverse effect on the FISH analysis (data not shown). Furthermore, two different automated algorithms for fusion discovery from RNA data did not detect the underlying gene fusion in any of these six cases. This may come down to the highly repetitive DNA sequences juxtaposing the breakpoint in *CIC*. In three cases, the underlying *CIC-DUX4* fusion could only be detected by manually reviewing the reads of these genes in IGV.

A more practicable method might be using a surrogate marker. Gene expression profiling revealed an up-regulation of ETS transcription factors (*ETV1* on chromosome 7p, *ETV4* on chromosome 17q, *ETV5* on chromosome 3q) in small blue round cell tumors with *CIC*-

Author Manuscript Author Manuscript Author Manuscript Author Manuscript

DUX4 fusion (47-50). Likewise, BCOR overexpression has been proposed as a potential biomarker for diagnosing small blue round cell tumors with *BCOR* alteration, although diagnostic pitfalls have already been recognized (37, 51).

In conclusion, array-based DNA-methylation molecular profiling is a robust method that proved extraordinary powerful for clarifying the diagnoses of a cohort of tumors initially deemed small blue round cell tumor not otherwise specified. Although it remains to be seen whether DNA-methylation may delineate sarcoma subtypes not investigated in this study, this approach already now can be highly useful in the diagnosis of Ewing sarcoma and mimics.

Supplementary Material

Refer to Web version on PubMed Central for supplementary material.

Acknowledgements

We thank Simone Kocher, Jochen Meyer and Antje Habel for excellent technical support. We also thank Dr. Meybrit Rasper and Regina Kloss from the CESS study group for helpful assistance. We thank the Tissue Bank of the National Center for Tumor Diseases Heidelberg for providing samples, and the Microarray unit of the Genomics and Proteomics Core Facility, German Cancer Research Center (DKFZ), for providing excellent methylation services.

This study was supported by a German Cancer Aid grant 70112499 (to CK, AvD) and grant 108128 (to UD); ERA-Net-TRANSCAN consortium, project number 01KT1310, and Euro Ewing Consortium EEC, project number EU-FP7 602856, both funded under the European Commission Seventh Framework Program FP7-HEALTH (to UD).

References

1. Alava Ed, Lessnick SL, Sorensen PH. Ewing Sarcoma, In: Fletcher CDM, Bridge JA, Hogendoorn PCW, Mertens F, (eds). WHO Classification of Tumours of Soft Tissue and Bone. International Agency for Research on Cancer (IARC): Lyon; 2013 pp 305–10.
2. Folpe AL, Hill CE, Parham DM, O'Shea PA, Weiss SW. Immunohistochemical detection of FLI-1 protein expression: a study of 132 round cell tumors with emphasis on CD99-positive mimics of Ewing's sarcoma/primitive neuroectodermal tumor. Am J Surg Pathol 2000;24:1657–62. [PubMed: 11117787]
3. Delattre O, Zucman J, Plougastel B, Desmaze C, Melot T, Peter M, Kovar H, Joubert I, de Jong P, Rouleau G, et al. Gene fusion with an ETS DNA-binding domain caused by chromosome translocation in human tumours. Nature 1992;359:162–5. [PubMed: 1522903]
4. Sorensen PH, Lessnick SL, Lopez-Terrada D, Liu XF, Triche TJ, Denny CT. A second Ewing's sarcoma translocation, t(21;22), fuses the EWS gene to another ETS-family transcription factor, ERG. Nat Genet 1994;6:146–51. [PubMed: 8162068]
5. Szuhai K, Ijszenga M, de Jong D, Karseladze A, Tanke HJ, Hogendoorn PC. The NFATc2 gene is involved in a novel cloned translocation in a Ewing sarcoma variant that couples its function in immunology to oncology. Clin Cancer Res 2009;15:2259–68. [PubMed: 19318479]
6. Sumegi J, Nishio J, Nelson M, Frayer RW, Perry D, Bridge JA. A novel t(4;22)(q31;q12) produces an EWSR1-SMARCA5 fusion in extraskeletal Ewing sarcoma/primitive neuroectodermal tumor. Mod Pathol 2011;24:333–42. [PubMed: 21113140]
7. Kawamura-Saito M, Yamazaki Y, Kaneko K, Kawaguchi N, Kanda H, Mukai H, Gotoh T, Motoi T, Fukayama M, Aburatani H, Takizawa T, Nakamura T. Fusion between CIC and DUX4 up-regulates PEA3 family genes in Ewing-like sarcomas with t(4;19)(q35;q13) translocation. Hum Mol Genet 2006;15:2125–37. [PubMed: 16717057]

Author Manuscript Author Manuscript Author Manuscript Author Manuscript

8. Pierron G, Tirode F, Lucchesi C, Reynaud S, Ballet S, Cohen-Gogo S, Perrin V, Coindre JM, Delattre O. A new subtype of bone sarcoma defined by BCOR-CCNB3 gene fusion. Nat Genet 2012;44:461–6. [PubMed: 22387997]

9. Italiano A, Sung YS, Zhang L, Singer S, Maki RG, Coindre JM, Antonescu CR. High prevalence of CIC fusion with double-homeobox (DUX4) transcription factors in EWSR1-negative undifferentiated small blue round cell sarcomas. Genes Chromosomes Cancer 2012;51:207–18. [PubMed: 22072439]

10. Specht K, Zhang L, Sung YS, Nucci M, Dry S, Vaiyapuri S, Richter GH, Fletcher CD, Antonescu CR. Novel BCOR-MAML3 and ZC3H7B-BCOR Gene Fusions in Undifferentiated Small Blue Round Cell Sarcomas. Am J Surg Pathol 2016;40:433–42. [PubMed: 26752546]

11. Antonescu C Round cell sarcomas beyond Ewing: emerging entities. Histopathology 2014;64:26–37. [PubMed: 24215322]

12. Reik W. Stability and flexibility of epigenetic gene regulation in mammalian development. Nature 2007;447:425–32. [PubMed: 17522676]

13. Straussman R, Nejman D, Roberts D, Steinfeld I, Blum B, Benvenisty N, Simon I, Yakhini Z, Cedar H. Developmental programming of CpG island methylation profiles in the human genome. Nat Struct Mol Biol 2009;16:564–71. [PubMed: 19377480]

14. Heyn H, Esteller M. DNA methylation profiling in the clinic: applications and challenges. Nat Rev Genet 2012;13:679–92. [PubMed: 22945394]

15. Johann PD, Erkek S, Zapatka M, Kerl K, Buchhalter I, Hovestadt V, Jones DT, Sturm D, Hermann C, Segura Wang M, Korshunov A, Rhyzova M, Grobner S, Brabetz S, Chavez L, Bens S, Groschel S, Kratochwil F, Wittmann A, Sieber L, Georg C, Wolf S, Beck K, Oyen F, Capper D, van Sluis P, Volckmann R, Koster J, Versteeg R, von Deimling A, Milde T, Witt O, Kulozik AE, Ebinger M, Shalaby T, Grotzer M, Sumerauer D, Zamecnik J, Mora J, Jabado N, Taylor MD, Huang A, Aronica E, Bertoni A, Radlwimmer B, Pietsch T, Schuller U, Schneppenheim R, Northcott PA, Korbel JO, Siebert R, Fruhwald MC, Lichter P, Eils R, Gajjar A, Hasselblatt M, Pfister SM, Kool M. Atypical Teratoid/Rhabdoid Tumors Are Comprised of Three Epigenetic Subgroups with Distinct Enhancer Landscapes. Cancer Cell 2016;29:379–93. [PubMed: 26923874]

16. Koelsche C, Hovestadt V, Jones DT, Capper D, Sturm D, Sahm F, Schrimpf D, Adeberg S, Bohmer K, Hagenlocher C, Mechtersheimer G, Kohlhof P, Muhleisen H, Beschorner R, Hartmann C, Braczynski AK, Mittelbronn M, Buslei R, Becker A, Grote A, Urbach H, Staszewski O, Prinz M, Hewer E, Pfister SM, von Deimling A, Reuss DE. Melanotic tumors of the nervous system are characterized by distinct mutational, chromosomal and epigenomic profiles. Brain Pathol 2015;25:202–8. [PubMed: 25399693]

17. Mahoney SE, Yao Z, Keyes CC, Tapscott SJ, Diede SJ. Genome-wide DNA methylation studies suggest distinct DNA methylation patterns in pediatric embryonal and alveolar rhabdomyosarcomas. Epigenetics 2012;7:400–8. [PubMed: 22419069]

18. Pajtler KW, Witt H, Sill M, Jones DT, Hovestadt V, Kratochwil F, Wani K, Tatevossian R, Punchihewa C, Johann P, Reimand J, Warnatz HJ, Ryzhova M, Mack S, Ramaswamy V, Capper D, Schweizer L, Sieber L, Wittmann A, Huang Z, van Sluis P, Volckmann R, Koster J, Versteeg R, Fults D, Toledano H, Avigad S, Hoffman LM, Donson AM, Foreman N, Hewer E, Zitterbart K, Gilbert M, Armstrong TS, Gupta N, Allen JC, Karajannis MA, Zagzag D, Hasselblatt M, Kulozik AE, Witt O, Collins VP, von Hoff K, Rutkowski S, Pietsch T, Bader G, Yaspo ML, von Deimling A, Lichter P, Taylor MD, Gilbertson R, Ellison DW, Aldape K, Korshunov A, Kool M, Pfister SM. Molecular Classification of Ependymal Tumors across All CNS Compartments, Histopathological Grades, and Age Groups. Cancer Cell 2015;27:728–43. [PubMed: 25965575]

19. Rohrich M, Koelsche C, Schrimpf D, Capper D, Sahm F, Kratz A, Reuss J, Hovestadt V, Jones DT, Bewerunge-Hudler M, Becker A, Weis J, Mawrin C, Mittelbronn M, Perry A, Mautner VF, Mechtersheimer G, Hartmann C, Okuducu AF, Arp M, Seiz-Rosenhagen M, Hanggi D, Heim S, Paulus W, Schittenhelm J, Ahmadi R, Herold-Mende C, Unterberg A, Pfister SM, von Deimling A, Reuss DE. Methylation-based classification of benign and malignant peripheral nerve sheath tumors. Acta Neuropathol 2016;131:877–87. [PubMed: 26857854]

20. Schwalbe EC, Williamson D, Lindsey JC, Hamilton D, Ryan SL, Megahed H, Garami M, Hauser P, Dembowska-Baginska B, Perek D, Northcott PA, Taylor MD, Taylor RE, Ellison DW, Bailey S, Clifford SC. DNA methylation profiling of medulloblastoma allows robust subclassification and

Author Manuscript Author Manuscript Author Manuscript Author Manuscript

improved outcome prediction using formalin-fixed biopsies. Acta Neuropathol 2013;125:359–71. [PubMed: 23291781]

21. Seki M, Nishimura R, Yoshida K, Shimamura T, Shiraishi Y, Sato Y, Kato M, Chiba K, Tanaka H, Hoshino N, Nagae G, Shiozawa Y, Okuno Y, Hosoi H, Tanaka Y, Okita H, Miyachi M, Souzaki R, Taguchi T, Koh K, Hanada R, Kato K, Nomura Y, Akiyama M, Oka A, Igarashi T, Miyano S, Aburatani H, Hayashi Y, Ogawa S, Takita J. Integrated genetic and epigenetic analysis defines novel molecular subgroups in rhabdomyosarcoma. Nat Commun 2015;6:7557. [PubMed: 26138366]
22. Sturm D, Orr BA, Toprak UH, Hovestadt V, Jones DTW, Capper D, Sill M, Buchhalter I, Northcott PA, Leis I, Ryzhova M, Koelsche C, Pfaff E, Allen SJ, Balasubramanian G, Worst BC, Pajtler KW, Brabetz S, Johann PD, Sahm F, Reimand J, Mackay A, Carvalho DM, Remke M, Phillips JJ, Perry A, Cowdrey C, Drissi R, Fouladi M, Giangaspero F, Lastowska M, Grajkowska W, Scheurlen W, Pietsch T, Hagel C, Gojo J, Lotsch D, Berger W, Slavc I, Haberler C, Jouvet A, Holm S, Hofer S, Prinz M, Keohane C, Fried I, Mawrin C, Scheie D, Mobley BC, Schniederjan MJ, Santi M, Buccoliero AM, Dahiya S, Kramm CM, von Bueren AO, von Hoff K, Rutkowski S, Herold-Mende C, Fruhwald MC, Milde T, Hasselblatt M, Wesseling P, Rossler J, Schuller U, Ebinger M, Schittenhelm J, Frank S, Grobholz R, Vajtai I, Hans V, Schneppenheim R, Zitterbart K, Collins VP, Aronica E, Varlet P, Puget S, Dufour C, Grill J, Figarella-Branger D, Wolter M, Schuhmann MU, Shalaby T, Grotzer M, van Meter T, Monoranu CM, Felsberg J, Reifenberger G, Snuderl M, Forrester LA, Koster J, Versteeg R, Volckmann R, van Sluis P, Wolf S, Mikkelsen T, Gajjar A, Aldape K, Moore AS, Taylor MD, Jones C, Jabado N, Karajannis MA, Eils R, Schlesner M, Lichter P, von Deimling A, Pfister SM, Ellison DW, Korshunov A, Kool M. New Brain Tumor Entities Emerge from Molecular Classification of CNS-PNETs. Cell 2016;164:1060–72. [PubMed: 26919435]
23. Sturm D, Witt H, Hovestadt V, Khuong-Quang DA, Jones DT, Konermann C, Pfaff E, Tonjes M, Sill M, Bender S, Kool M, Zapatka M, Becker N, Zucknick M, Hielscher T, Liu XY, Fontebasso AM, Ryzhova M, Albrecht S, Jacob K, Wolter M, Ebinger M, Schuhmann MU, van Meter T, Fruhwald MC, Hauch H, Pekrun A, Radlwimmer B, Niehues T, von Komorowski G, Durken M, Kulozik AE, Madden J, Donson A, Foreman NK, Drissi R, Fouladi M, Scheurlen W, von Deimling A, Monoranu C, Roggendorf W, Herold-Mende C, Unterberg A, Kramm CM, Felsberg J, Hartmann C, Wiestler B, Wick W, Milde T, Witt O, Lindroth AM, Schwartzentruber J, Faury D, Fleming A, Zakrzewska M, Liberski PP, Zakrzewski K, Hauser P, Garami M, Klekner A, Bognar L, Morrissy S, Cavalli F, Taylor MD, van Sluis P, Koster J, Versteeg R, Volckmann R, Mikkelsen T, Aldape K, Reifenberger G, Collins VP, Majewski J, Korshunov A, Lichter P, Plass C, Jabado N, Pfister SM. Hotspot mutations in H3F3A and IDH1 define distinct epigenetic and biological subgroups of glioblastoma. Cancer Cell 2012;22:425–37. [PubMed: 23079654]
24. Hovestadt V, Remke M, Kool M, Pietsch T, Northcott PA, Fischer R, Cavalli FM, Ramaswamy V, Zapatka M, Reifenberger G, Rutkowski S, Schick M, Bewerunge-Hudler M, Korshunov A, Lichter P, Taylor MD, Pfister SM, Jones DT. Robust molecular subgrouping and copy-number profiling of medulloblastoma from small amounts of archival tumour material using high-density DNA methylation arrays. Acta Neuropathol 2013;125:913–6. [PubMed: 23670100]
25. Sahm F, Schrimpf D, Stichel D, Jones DTW, Hielscher T, Schefzyk S, Okonechnikov K, Koelsche C, Reuss DE, Capper D, Sturm D, Wirsching HG, Berghoff AS, Baumgarten P, Kratz A, Huang K, Wefers AK, Hovestadt V, Sill M, Ellis HP, Kurian KM, Okuducu AF, Jungk C, Drueschler K, Schick M, Bewerunge-Hudler M, Mawrin C, Seiz-Rosenhagen M, Ketter R, Simon M, Westphal M, Lamszus K, Becker A, Koch A, Schittenhelm J, Rushing EJ, Collins VP, Brehmer S, Chavez L, Platten M, Hanggi D, Unterberg A, Paulus W, Wick W, Pfister SM, Mittelbronn M, Preusser M, Herold-Mende C, Weller M, von Deimling A. DNA methylation-based classification and grading system for meningioma: a multicentre, retrospective analysis. Lancet Oncol 2017;18:682–94. [PubMed: 28314689]
26. Gaspar N, Hawkins DS, Dirksen U, Lewis IJ, Ferrari S, Le Deley MC, Kovar H, Grimer R, Whelan J, Claude L, Delattre O, Paulussen M, Picci P, Sundby Hall K, van den Berg H, Ladenstein R, Michon J, Hjorth L, Judson I, Luksch R, Bernstein ML, Marec-Berard P, Brennan B, Craft AW, Womer RB, Juergens H, Oberlin O. Ewing Sarcoma: Current Management and Future Approaches Through Collaboration. J Clin Oncol 2015;33:3036–46. [PubMed: 26304893]

Author Manuscript Author Manuscript Author Manuscript Author Manuscript

27. Ladenstein R, Potschger U, Le Deley MC, Whelan J, Paulussen M, Oberlin O, van den Berg H, Dirksen U, Hjorth L, Michon J, Lewis I, Craft A, Jurgens H. Primary disseminated multifocal Ewing sarcoma: results of the Euro-EWING 99 trial. J Clin Oncol 2010;28:3284–91. [PubMed: 20547982]

28. Le Deley MC, Paulussen M, Lewis I, Brennan B, Ranft A, Whelan J, Le Teuff G, Michon J, Ladenstein R, Marec-Berard P, van den Berg H, Hjorth L, Wheatley K, Judson I, Juergens H, Craft A, Oberlin O, Dirksen U. Cyclophosphamide compared with ifosfamide in consolidation treatment of standard-risk Ewing sarcoma: results of the randomized noninferiority Euro-EWING99-R1 trial. J Clin Oncol 2014;32:2440–8. [PubMed: 24982464]

29. Kim D, Salzberg SL. TopHat-Fusion: an algorithm for discovery of novel fusion transcripts. Genome Biol 2011;12:R72. [PubMed: 21835007]

30. McPherson A, Hormozdiari F, Zayed A, Giuliany R, Ha G, Sun MG, Griffith M, Heravi Moussavi A, Senz J, Melnyk N, Pacheco M, Marra MA, Hirst M, Nielsen TO, Sahinalp SC, Huntsman D, Shah SP. deFuse: an algorithm for gene fusion discovery in tumor RNA-Seq data. PLoS Comput Biol 2011;7:e1001138. [PubMed: 21625565]

31. Robinson JT, Thorvaldsdottir H, Winckler W, Guttman M, Lander ES, Getz G, Mesirov JP. Integrative genomics viewer. Nat Biotechnol 2011;29:24–6. [PubMed: 21221095]

32. Braun M, Stomper J, Boehm D, Vogel W, Scheble VJ, Wernert N, Shaikhibrahim Z, Fend F, Kristiansen G, Perner S. Improved method of detecting the ERG gene rearrangement in prostate cancer using combined dual-color chromogenic and silver in situ hybridization. J Mol Diagn 2012;14:322–7. [PubMed: 22642898]

33. Sahm F, Schrimpf D, Jones DT, Meyer J, Kratz A, Reuss D, Capper D, Koelsche C, Korshunov A, Wiestler B, Buchhalter I, Milde T, Selt F, Sturm D, Kool M, Hummel M, Bewerunge-Hudler M, Mawrin C, Schuller U, Jungk C, Wick A, Witt O, Platten M, Herold-Mende C, Unterberg A, Pfister SM, Wick W, von Deimling A. Next-generation sequencing in routine brain tumor diagnostics enables an integrated diagnosis and identifies actionable targets. Acta Neuropathol 2016;131:903–10. [PubMed: 26671409]

34. Wang L, Motoi T, Khanin R, Olshen A, Mertens F, Bridge J, Dal Cin P, Antonescu CR, Singer S, Hameed M, Bovee JV, Hogendoorn PC, Socci N, Ladanyi M. Identification of a novel, recurrent HEY1-NCOA2 fusion in mesenchymal chondrosarcoma based on a genome-wide screen of exon-level expression data. Genes Chromosomes Cancer 2012;51:127–39. [PubMed: 22034177]

35. Arbajian E, Magnusson L, Brosjo O, Wejde J, Folpe AL, Nord KH, Mertens F. A benign vascular tumor with a new fusion gene: EWSR1-NFATC1 in hemangioma of the bone. Am J Surg Pathol 2013;37:613–6. [PubMed: 23480895]

36. Sadri N, Barroeta J, Pack SD, Abdullaev Z, Chatterjee B, Puthiyaveettil R, Brooks JS, Barr FG, Zhang PJ. Malignant round cell tumor of bone with EWSR1-NFATC2 gene fusion. Virchows Arch 2014;465:233–9. [PubMed: 24993903]

37. Kao YC, Sung YS, Zhang L, Jungbluth AA, Huang SC, Argani P, Agaram NP, Zin A, Alaggio R, Antonescu CR. BCOR Overexpression Is a Highly Sensitive Marker in Round Cell Sarcomas With BCOR Genetic Abnormalities. Am J Surg Pathol 2016;40:1670–8. [PubMed: 27428733]

38. Kao YC, Sung YS, Zhang L, Huang SC, Argani P, Chung CT, Graf NS, Wright DC, Kellie SJ, Agaram NP, Ludwig K, Zin A, Alaggio R, Antonescu CR. Recurrent BCOR Internal Tandem Duplication and YWHAE-NUTM2B Fusions in Soft Tissue Undifferentiated Round Cell Sarcoma of Infancy: Overlapping Genetic Features With Clear Cell Sarcoma of Kidney. Am J Surg Pathol 2016;40:1009–20. [PubMed: 26945340]

39. Ueno-Yokohata H, Okita H, Nakasato K, Akimoto S, Hata J, Koshinaga T, Fukuzawa M, Kiyokawa N. Consistent in-frame internal tandem duplications of BCOR characterize clear cell sarcoma of the kidney. Nat Genet 2015;47:861–3. [PubMed: 26098867]

40. Argani P, Kao YC, Zhang L, Bacchi C, Matoso A, Alaggio R, Epstein JI, Antonescu CR. Primary Renal Sarcomas With BCOR-CCNB3 Gene Fusion: A Report of 2 Cases Showing Histologic Overlap With Clear Cell Sarcoma of Kidney, Suggesting Further Link Between BCOR-related Sarcomas of the Kidney and Soft Tissues. Am J Surg Pathol 2017;41:1702–12. [PubMed: 28817404]

41. Yoshida Y, Nobusawa S, Nakata S, Nakada M, Arakawa Y, Mineharu Y, Sugita Y, Yoshioka T, Araki A, Sato Y, Takeshima H, Okada M, Nishi A, Yamazaki T, Kohashi K, Oda Y, Hirato J,

Author Manuscript Author Manuscript Author Manuscript Author Manuscript

Yokoo H. CNS high-grade neuroepithelial tumor with BCOR internal tandem duplication: a comparison with its counterparts in the kidney and soft tissue. Brain Pathol 2017.

42. Huang SC, Zhang L, Sung YS, Chen CL, Kao YC, Agaram NP, Antonescu CR. Secondary EWSR1 gene abnormalities in SMARCB1-deficient tumors with 22q11–12 regional deletions: Potential pitfalls in interpreting EWSR1 FISH results. Genes Chromosomes Cancer 2016;55:767–76. [PubMed: 27218413]
43. Solomon DA, Brohl AS, Khan J, Miettinen M. Clinicopathologic features of a second patient with Ewing-like sarcoma harboring CIC-FOXO4 gene fusion. Am J Surg Pathol 2014;38:1724–5. [PubMed: 25321332]
44. Sugita S, Arai Y, Tonooka A, Hama N, Totoki Y, Fujii T, Aoyama T, Asanuma H, Tsukahara T, Kaya M, Shibata T, Hasegawa T. A novel CIC-FOXO4 gene fusion in undifferentiated small round cell sarcoma: a genetically distinct variant of Ewing-like sarcoma. Am J Surg Pathol 2014;38:1571–6. [PubMed: 25007147]
45. Antonescu CR, Owosho AA, Zhang L, Chen S, Deniz K, Huryn JM, Kao YC, Huang SC, Singer S, Tap W, Schaefer IM, Fletcher CD. Sarcomas With CIC-rearrangements are a Distinct Pathologic Entity With Aggressive Outcome: A Clinicopathologic and Molecular Study of 115 Cases. Am J Surg Pathol 2017.
46. Yoshida A, Arai Y, Kobayashi E, Yonemori K, Ogura K, Hama N, Mukai W, Motoi T, Kawai A, Shibata T, Hiraoka N. CIC break-apart fluorescence in-situ hybridization misses a subset of CIC-DUX4 sarcomas: a clinicopathological and molecular study. Histopathology 2017;71:461–9. [PubMed: 28493604]
47. Kao YC, Sung YS, Chen CL, Zhang L, Dickson BC, Swanson D, Vaiyapuri S, Latif F, Alholle A, Huang SC, Hornick JL, Antonescu CR. ETV transcriptional upregulation is more reliable than RNA sequencing algorithms and FISH in diagnosing round cell sarcomas with CIC gene rearrangements. Genes Chromosomes Cancer 2017;56:501–10. [PubMed: 28233365]
48. Specht K, Sung YS, Zhang L, Richter GH, Fletcher CD, Antonescu CR. Distinct transcriptional signature and immunoprofile of CIC-DUX4 fusion-positive round cell tumors compared to EWSR1-rearranged Ewing sarcomas: further evidence toward distinct pathologic entities. Genes Chromosomes Cancer 2014;53:622–33. [PubMed: 24723486]
49. Le Guellec S, Velasco V, Perot G, Watson S, Tirode F, Coindre JM. ETV4 is a useful marker for the diagnosis of CIC-rearranged undifferentiated round-cell sarcomas: a study of 127 cases including mimicking lesions. Mod Pathol 2016;29:1523–31. [PubMed: 27562494]
50. Smith SC, Palanisamy N, Martin E, Almenara J, McHugh JB, Choi EK, Lucas DR, Betz BL, Thomas D, Patel RM. The utility of ETV1, ETV4 and ETV5 RNA in-situ hybridization in the diagnosis of CIC-DUX sarcomas. Histopathology 2017;70:657–63. [PubMed: 27790742]
51. Kao YC, Sung YS, Zhang L, Kenan S, Singer S, Tap WD, Swanson D, Dickson BC, Antonescu CR. BCOR upregulation in a poorly differentiated synovial sarcoma with SS18L1-SSX1 fusion-A pathologic and molecular pitfall. Genes Chromosomes Cancer 2017;56:296–302. [PubMed: 27914109]

Author Manuscript Author Manuscript Author Manuscript Author Manuscript

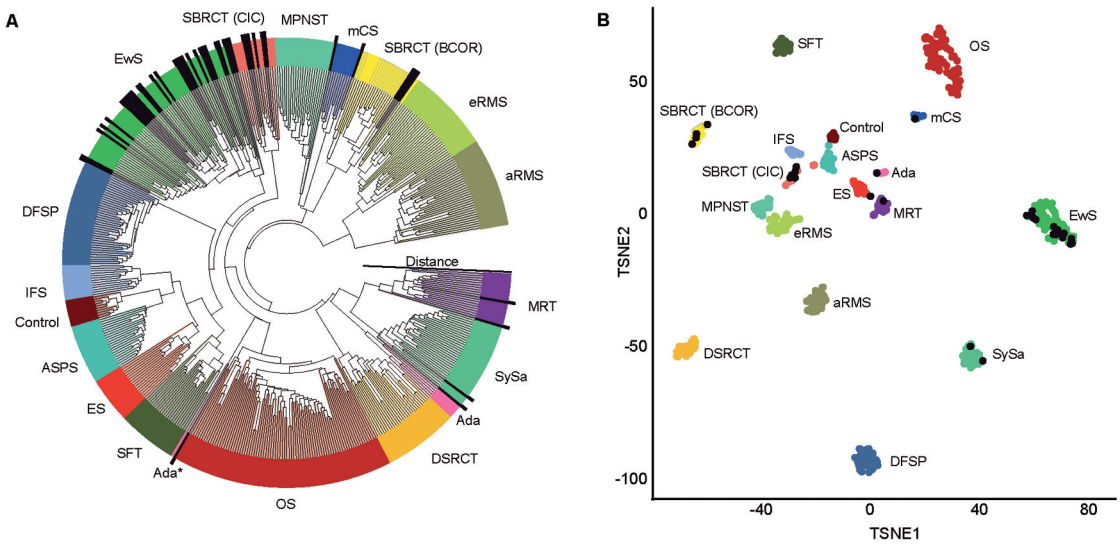

Figure 1. Assignment of 30 small blue round cell tumors not otherwise specified to methylation groups of reference sarcoma sets.

(A) - unsupervised hierarchical clustering analysis, and (B) - t-distributed stochastic neighbor embedding using the 10,000 most variable DNA-methylation probes of array-generated DNA-methylation profiles from the Illumina Infinium HumanMethylation450 or EPIC BeadChip (Illumina, San Diego, USA). Black bars/circles indicate the positions of the 30 small blue round cell tumors not otherwise specified.

Abbreviations: Ada = adamantinoma (* suspect); ASPS = alveolar soft part sarcoma; mCS = mesenchymal chondrosarcoma; CCSK = clear cell sarcoma of the kidney; CT = control tissue of non-neoplastic inflammatory origin; OS = conventional osteosarcoma; DFSP - dermatofibrosarcoma protuberans ; DSRCT = desmoplastic small round cell tumor; ES = epithelioid sarcoma; EwS = Ewing sarcoma; IFS = infantile fibrosarcoma; MPNST = malignant peripheral nerve sheath tumor; MRT = malignant rhabdoid tumor; eRMS = embryonal rhabdomyosarcoma; aRMS = alveolar rhabdomyosarcoma; SBRCT (BCOR) = small blue round cell tumor with *BCOR* alteration (*BCOR-CCNB3* fusion = yellow; internal tandem duplication = yellow with greyish contour); SBRCT (CIC) = small blue round cell tumor with *CIC* alteration; SFT = solitary fibrous tumor; SySa = synovial sarcoma

Author Manuscript Author Manuscript Author Manuscript Author Manuscript

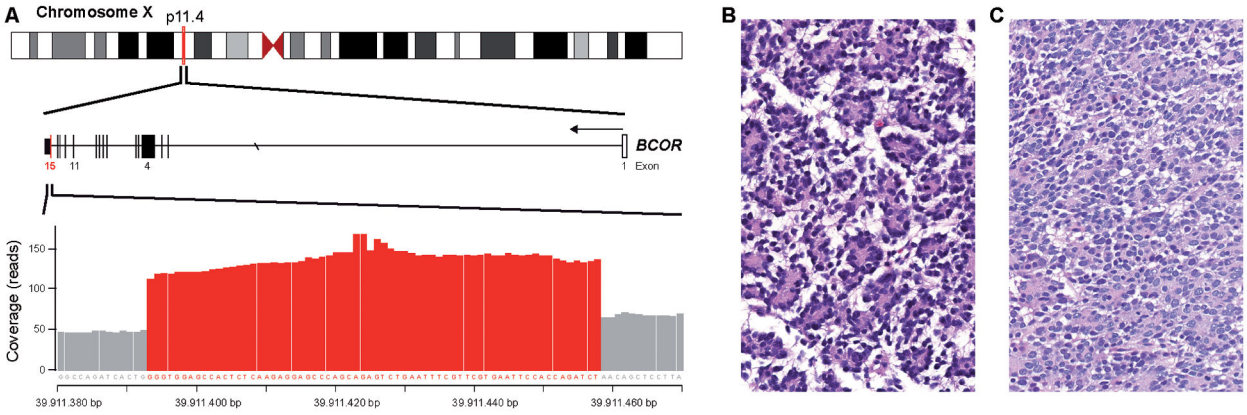

Figure 2. *BCOR* internal tandem duplication in a skull tumor of an infant.

The genomic footprint of *BCOR* is depicted (A). The duplicated 66 bp sequence in Exon 15, which encodes for the PCGF Ub-like fold discriminator (PUFD) domain at the C-terminus of BCOR, is recognizable by a sharply demarcated doubling of the coverage rate. The tumor cells focally present with a vacuolated cytoplasm (B). Rosette formations are prominent in some areas (C).

Author Manuscript Author Manuscript Author Manuscript Author Manuscript

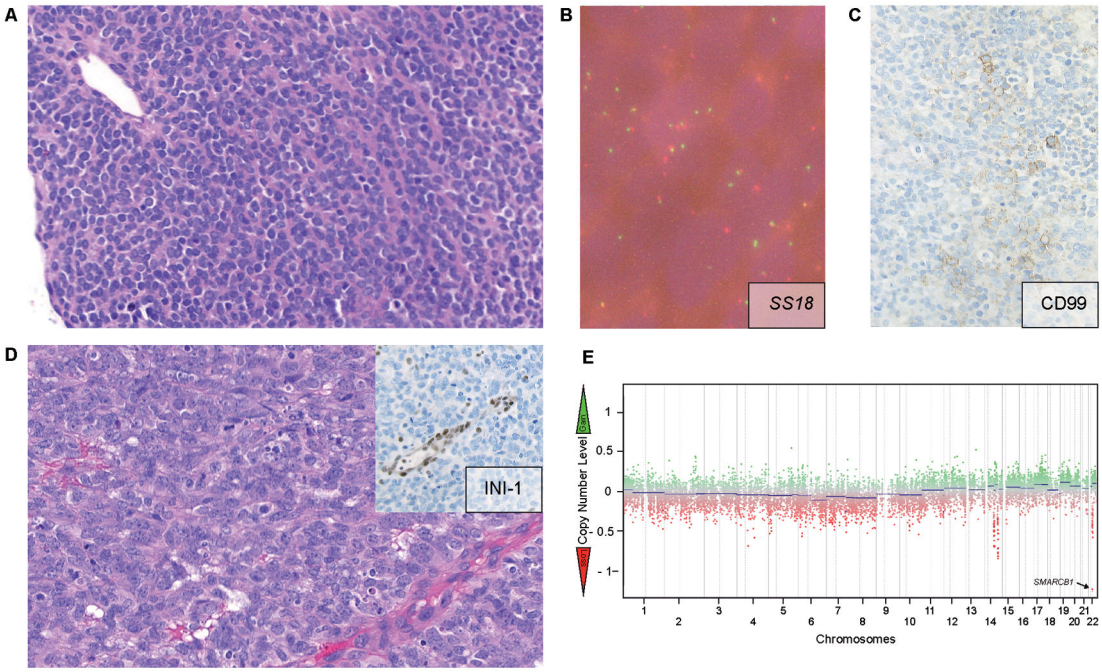

Figure 3. Histologic phenotypes of two representative Ewing-like sarcomas.

Case 83172 (A-C) represents a poorly differentiated synovial sarcoma exhibiting a small blue round cell phenotype (A). FISH analysis revealed a *SS18* break-apart signal indicated by two separated green and red signals (B). Interestingly, some tumor cells express CD99 (C). Case 94172 (D, E) exhibits an epithelioid to rhabdoid phenotype (D). Nuclear INI-1 expression is lost (D; inlet). Copy number analysis demonstrated a loss on chromosome arm 19q involving the *SMARCB1* locus (E).

Author Manuscript Author Manuscript Author Manuscript Author Manuscript

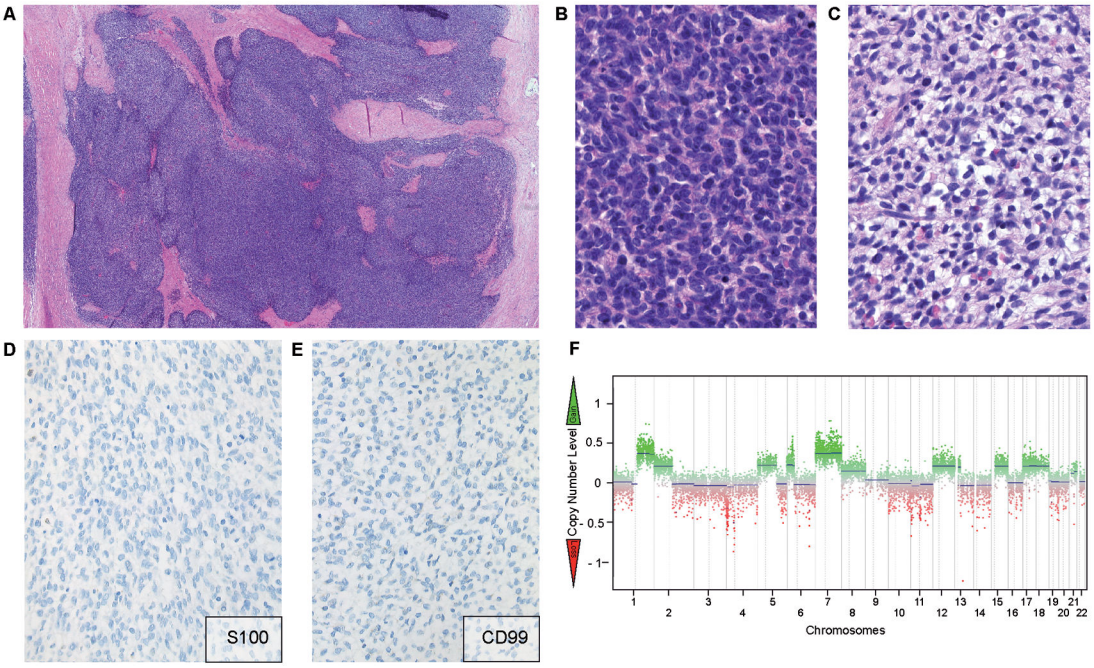

Figure 4. Histological phenotype of an unusual mesenchymal chondrosarcoma.

Case 95322 shows an organoid growth pattern at low-power view (A). The small round tumor cells are arranged in sheets (B). In less cellular parts the tumor shows a vague reticulated growth pattern (C). The tumor is almost negative for S100 (D) and CD99 (E). A copy number analysis demonstrates several whole-chromosome gains (F).

Author Manuscript Author Manuscript Author Manuscript Author Manuscript

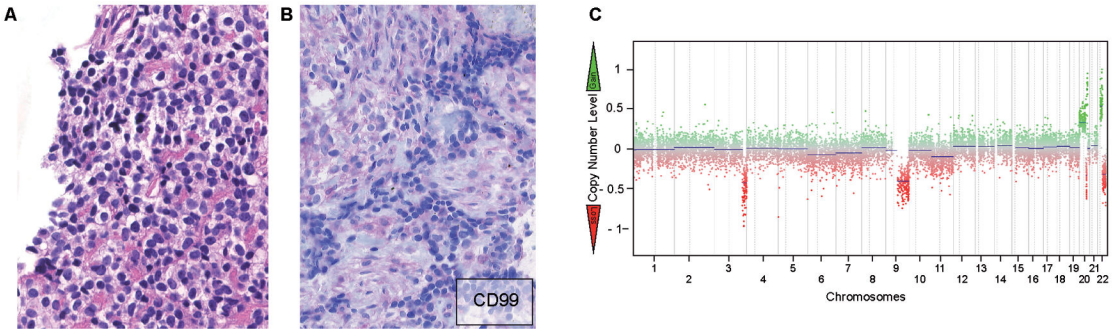

Figure 5. Histologic phenotype of case with an *EWSR1-NFATC2* gene fusion.

Case 97480 is a highly cellular round cell tumor with an indistinctive growth pattern (A). The tumor cells faintly express CD99 (B). A copy number analysis demonstrates complex chromosomal alterations, e.g. on chromosome 22, on an otherwise relatively balanced background (C).

Author Manuscript Author Manuscript Author Manuscript Author Manuscript

Table 1.

DNA-methylation based prediction and genetic validation.

Case	Methylation class	Validation results	Method
83218	EwS	*EWSR1-FLI1* (E7-E7)	FISH (ND), RT-PCR (neg), NGS (pos)
94168	EwS	*EWSR1-FLI1* (E7-E7)	FISH (NA), RT-PCR (NA), NGS (pos)
94170	EwS	*EWSR1-FLI1* (E7-E7)	FISH (NA), RT-PCR (NA), NGS (pos)
97476	EwS	*FLI1-EWSR1* (E7-E8)	FISH (neg), RT-PCR (NA, NGS (pos)
95332	EwS	*EWSR1-FEV* (E7-E2)	FISH (ND), RT-PCR (neg), NGS (pos)
83240	EwS	*EWSR1-ETV1* (E16-E9)	FISH (ND), RT-PCR (neg), NGS (pos)
94186	EwS	*EWSR1-FLI1*	FISH (ND), RT-PCR (neg), NGS (pos)
97474	EwS	*EWSR1-FLI1*	FISH (ND), RT-PCR (neg), NGS (pos)
83224	EwS	*EWSR1* break-apart	FISH (pos), RT-PCR (neg), NGS (neg)
83226	EwS	*EWSR1* break-apart	FISH (pos), RT-PCR (neg), NGS (neg)
83232	EwS	*EWSR1* break-apart	FISH (pos), RT-PCR (neg), NGS (neg)
94178	EwS	*FUS* break-apart	FISH (pos), RT-PCR (neg), NGS (neg)
94182	EwS	no finding	FISH (NA), RT-PCR (NA), NGS (neg)
94192	EwS	non-determinable	FISH (ND), RT-PCR (neg), NGS (ND)
83220	SBRCT (CIC)	*CIC-DUX4*	FISH (pos), NGS (pos)
95324	SBRCT (CIC)	*CIC-DUX4*	FISH (pos), NGS (pos)
97478	SBRCT (CIC)	*CIC-DUX4*	FISH (neg), NGS (pos)
83172	SBRCT (CIC)	*CIC break*-apart	FISH (pos), NGS (neg)
95310	SBRCT (CIC)	*CIC* break-apart	FISH (pos), NGS (neg)
94194	SBRCT (CIC)	no finding	FISH (NA), NGS (neg)
85094	SBRCT (BCOR)	*BCOR-CCNB3* (E15-E5)	RT-PCR (pos), NGS (pos)
85096	SBRCT (BCOR)	*BCOR-CCNB3* (E15-E5)	RT-PCR (pos), NGS (pos)
95330	SBRCT (BCOR)	*BCOR-CCNB3* (E15-E5)	RT-PCR (pos), NGS (pos)
96930	SBRCT (BCOR)	*BCOR* ITD	RT-PCR (neg), NGS (neg), NGS-P (pos)
83174	SySa	*SS18* break-apart	FISH (pos)
95328	SySa	*SS18* break-apart	FISH (pos)
94172	MRT	*SMARCB1* deficiency	CNP, IHC
95326	MRT	*SMARCB1* deficiency	CNP, IHC
97480	Ada (−/+)	*EWSR1-NFATC2* (E8-E3)	FISH (pos), RT-PCR (neg), NGS (pos)
95322	mCS (−/+)	no finding	FISH (neg), RT-PCR (neg), NGS (neg)

Abbreviations: EwS = Ewing sarcoma; SBRCT (CIC) = small blue round cell tumor with *CIC* alteration; SBRCT (BCOR) = small blue round cell tumor with *BCOR* alteration; SySa = synovial sarcoma; MRT = malignant rhabdoid tumor; mCS = mesenchymal chondrosarcoma; Ada = adamantinoma; NGS = total RNA next generation sequencing; CNP = copy number profile; IHC = immunohistochemistry